Compact Dual-Band Rectifier with Self-Matched Branches Using Comprehensive Impedance Control

Adel Barakat[1], Ramesh K Pokharel[1], and Willy Jordan[2]

[1]Affiliation not available
[2]Kyushu University

February 04, 2025

Abstract

The use of multi-band matching for rectifiers leads to design complexity. Instead, recent advancements suggested self-matched branches combined in parallel to enable multiband operation. However, this method controls only the imaginary part. In this letter, we propose an efficient dual-band rectifier with compact realization. The rectifier consists of two self-matched parallel branches. Each branch provides comprehensive impedance control over real and imaginary parts in the corresponding band independent of the design frequency. The branch impedance matching is analyzed theoretically, and design equations are presented. To verify the proposed theory, a compact dual-band rectifier was fabricated with a compact area of only 0.42 cm2 after excluding the area required for the RF connector. The measured RF-DC power conversion efficiency (PCE) was $> 50\%$ for input power (???) ranging from -5.5 dBm to 11 dBm at 390 MHz with a peak of 69%. Also, the PCE was $> 50\%$ for ??? ranging from -4 dBm to 12 dBm at 690 MHz with a peak of 68%. The fabricated rectifier operates with a wide load range from 0.5 KΩ to 3 KΩ with PCE $> 50\%$ at both bands when ??? = ? dBm.

Compact Dual-Band Rectifier with Self-Matched Branches Using Comprehensive Impedance Control

Adel Barakat, *Member, IEEE*, and Ramesh K. Pokharel, *Member, IEEE*

***Abstract*—The use of multi-band matching for rectifiers leads to design complexity. Instead, recent advancements suggested self-matched branches combined in parallel to enable multiband operation. However, this method controls only the imaginary part. In this letter, we propose an efficient dual-band rectifier with compact realization. The rectifier consists of two self-matched parallel branches. Each branch provides comprehensive impedance control over real and imaginary parts in the corresponding band independent of the design frequency. The branch impedance matching is analyzed theoretically, and design equations are presented. To verify the proposed theory, a compact dual-band rectifier was fabricated with a compact area of only 0.42 cm² after excluding the area required for the RF connector. The measured RF-DC power conversion efficiency (PCE) was > 50% for input power (P_{in}) ranging from -5.5 dBm to 11 dBm at 390 MHz with a peak of 69%. Also, the PCE was > 50% for P_{in} ranging from -4 dBm to 12 dBm at 690 MHz with a peak of 68%. The fabricated rectifier operates with a wide load range from 0.5 KΩ to 3 KΩ with PCE > 50% at both bands when P_{in} = 5 dBm.**

***Index Terms*—Dual-band, Input Impedance, Low power, Self-matched, Rectifier, Wireless Power Transfer.**

I. INTRODUCTION

RECTIFIERS are the real bottleneck in achieving an efficient wireless power transfer (WPT) system for the Internet of Things (IoT) applications, including vital signs tracking for health monitoring, gas leakage detection for safety control, temperature, and humidity sensing for environmental management, and more. Recent scenarios for in-door WPT applications suggest that battery-less IoT sensors can be powered wirelessly through a far-field antenna. In such cases, the available RF power at the rectifier input may be a few milliwatts or less. Thus, efficient rectifiers for low input power are desired.

Achieving optimal performance in rectifiers critically depends on matching the RF input to the input impedance of the diode. This matching process is crucial as it directly influences the rectifier's RF-DC power conversion efficiency (PCE). Typically, at an available input power level, there is a trade-off between maximizing peak PCE and maintaining sufficient bandwidth (BW) for the desired application. This trade-off is particularly notable in scenarios with varying operating frequencies or where high PCE across a wide bandwidth is necessary. Considering these factors, rectifiers development focus was into two main directions: 1) multi-band impedance matching [1], [2], [3], [4], [5], [6], [7], [8], [9], [10], [11], [12], and 2) wide-band impedance matching [13], [14], [15], [16], [17], [18], [19], [20], [21], [22], [23], [24]. Although wideband may be desirable, it is associated with the requirement of relatively high input power to achieve a feasible level of PCE.

Recent advances in rectification techniques targeted to eliminate the need for a matching circuit or to have a simple one. A conjugate matching technique was employed in [9] for matching network elimination with triple-band operation. However, the antenna design complexity was greatly affected as the input impedance of the diode needed to be considered for each band. A multiband rectifier with self-matched branches [6] was proposed. Nonetheless, the equivalent input resistance of the diode depends on the design frequency. Hence, this method [6] can control only the imaginary part. In this letter, we propose a dual-band rectifier with comprehensive impedance control to maximize the PCE at any operating frequency. Also, lumped elements are used to ensure compact size.

II. PROPOSED TECHNIQUE

A. Analysis

The schematics of the conventional [6] and proposed self-matched rectifier are shown in Fig. 1(a) and 1(b), respectively. In both cases, at each frequency band, the self-matched structure consists of a diode and a series inductor. In the proposed case, an additional capacitor is proposed in parallel to the diode to offer comprehensive impedance control. Both designs can achieve a zero-input reactance at an arbitrary frequency of the loading elements. However, as shown in Fig. 1(c), the input resistance of the conventional self-matched rectifier increases when designed to operate at a lower operating frequency. In the proposed case a 50 Ω matching can be achieved by proper design of the series inductor and capacitor. In Fig. 1(c), f_{max} represents the maximum frequency at which an arbitrary input resistance, R_{in}, can be designed, 50 Ω in this work, due to the internal capacitance and other intrinsic parameters of the used diode at an available input power level and R_L.

This work was supported in part by the Japan Society for the Promotion of Science (JSPS) KAKENHI under Grant 22K14260, and in part by the activities of VLSI Design and Education Center (VDEC), The University of Tokyo, in collaboration with Keysight Technologies Japan, Ltd. *(Corresponding author: A. Barakat).*

The authors are with I&E Visionaries Department, Faculty of Information Science and Electrical Engineering, Kyushu University, Fukuoka 819-0001, Japan (e-mail: barakat@ed.kyushu-u.ac.jp, pokharel@ed.kyushu-u.ac.jp).

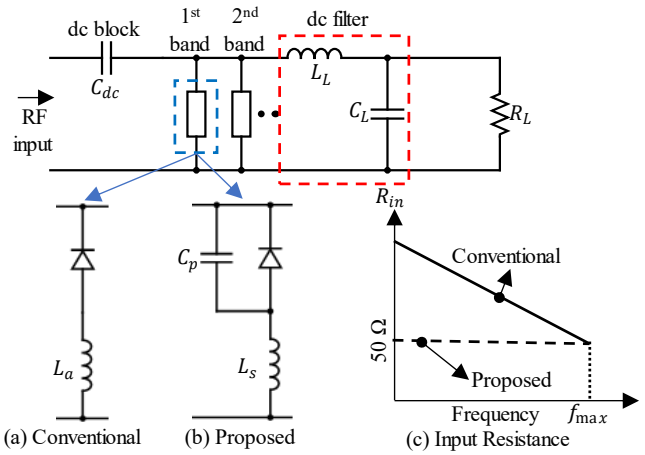

Fig. 1. Multi-band rectifier with sel-matched branches. (a) Conventional structure [6]. (b) Proposed structure. (c) Comparison between input resistance, R_{in}, in both cases where f_{max} represents the maximum frequency at which a specified R_{in} can be achieved.

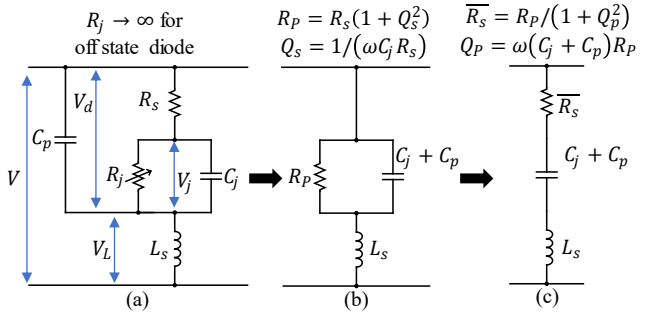

Fig. 2. Equivalent circuit of the proposed self-matched rectifier. (a) Initial circuit. (b) Circuit at off-state condition. (b) Final circuit at off-state condition.

The equivalent circuit of the proposed self-matched rectifier is shown in Fig. 2(a). The voltage across this self-matched structure can be expressed as (1) where V_o, V_{DP}, and V_{LP} are the DC output voltage, the peak voltage across the diode, and the peak voltage across the inductor.

$$V = V_d + V_L = -V_o + V_{DP}\cos\omega t + V_{LP}\cos\omega t \tag{1}$$

The junction voltage varies based on the on/off condition and can be expressed as (2) where V_{j0} and V_{j1} are the DC component and the peak of the AC component of the junction voltage. V_f is the diode's built-in voltage when the diode state is on. Also, θ is the phase delay between the input voltage and the junction voltage. Following a similar procedure for the on-state of the diode in [6], [13], the turn-on angle, $\emptyset_{on}$, should satisfy the condition in (3).

$$V_j = \begin{cases} -V_{j0} + V_{j1}\cos(\omega t - \theta), & \text{off state} \\ V_f, & \text{on state} \end{cases} \tag{2}$$

$$\tan\emptyset_{on} - \emptyset_{on} = \frac{\pi R_s}{R_L(1 + V_f/V_o)} \tag{3}$$

When the diode is reverse biased the junction resistance, R_j, is very high and acts as an open circuit. The typical values of junction capacitance, C_j, is a few hundred femto-Farads and of the series resistance, R_s, is a few ohms. So, their corresponding series quality factor, $Q_s = 1/(\omega C_j R_s)$, is relatively large. Consequently, the equivalent circuit can be re-drawn as shown in Fig. 2(b) where $R_P = R_s(1 + Q_s^2)$. Furthermore, the equivalent circuit can be further simplified as shown in Fig. 2(c) considering that $\overline{R_s}$, calculated using (4), is the overall series resistance and $Q_P = \omega(C_j + C_p)R_P$ is the quality factor of the parallel combination of R_P and $C_j + C_p$.

$$\overline{R_s} = \frac{R_P}{(1+Q_P^2)} = \frac{R_s(1+Q_s^2)}{(1+Q_P^2)} \tag{4}$$

Furthermore, following a similar analysis for the off state of the diode in [6], [13], the input impedance can be expressed as

$$Z_{in} = \frac{\pi\overline{R_s}A + j\left((A^2 + \omega^2B^2)\omega L_s - \pi\overline{R_s}\omega B\right)}{A^2 + \omega^2B^2} \tag{5}$$

and

$$A = \emptyset_{on} - \sin\emptyset_{on}\cos\emptyset_{on} \tag{6a}$$

$$B = \overline{R_s}(C_j + C_p)(\pi - A) \tag{6b}$$

At resonance, the reactance in (4) will vanish following the condition:

$$(A^2 + \omega^2B^2)L_s = \pi\overline{R_s}B \tag{7}$$

Correspondingly, Z_{in} will become pure resistive and, by substituting (7) in (5), it can be rewritten as

$$Z_{in} = \frac{A}{B} \times L_s = \frac{A}{\overline{R_s}(\pi - A)} \times \frac{L_s}{C_j + C_p} \tag{8}$$

Equation (8) shows that, in the proposed method, the impedance is pure real and can be controlled to an arbitrary value, by proper selection of L_s and C_p. To elaborate more on this finding, the input resistance and corresponding resonance frequency are designed and plotted against the loading elements for the conventional and proposed method as shown in Fig. 3(a) and 3(b), respectively. The SMS7621 diode (B_v = 3 V, V_f = 0.51 V, R_s = 12 Ω, and C_j = 0.1 pF) was utilized in this work. Simulations were done using the Advanced Design System (ADS).

In the conventional design method, L_a value defines the resonance frequency. But it has no control over the value of R_{in}. The reason behind this can be understood by setting $L_s = L_a$ and $C_p = 0$ in (8). Consequently, the lower the design resonance frequency, the larger the required value of L_a that leads to a larger value of R_{in} as shown in Fig. 3(a). Instead, in the proposed design method, the introduction of C_p added another degree of freedom. This allowed for the simultaneous design of both the frequency and R_{in} as shown in Fig. 3(b).

B. Design example of a dual-band rectifier

Based on the analysis in section II-B, a dual-band rectifier is designed for operation at 400 MHz and 700 MHz with an assumed DC output load of 2 KΩ. The layout of this proposed dual-band rectifier is shown in Fig. 4 and the optimized circuit elements based on (7) and (8) are listed in Table II.

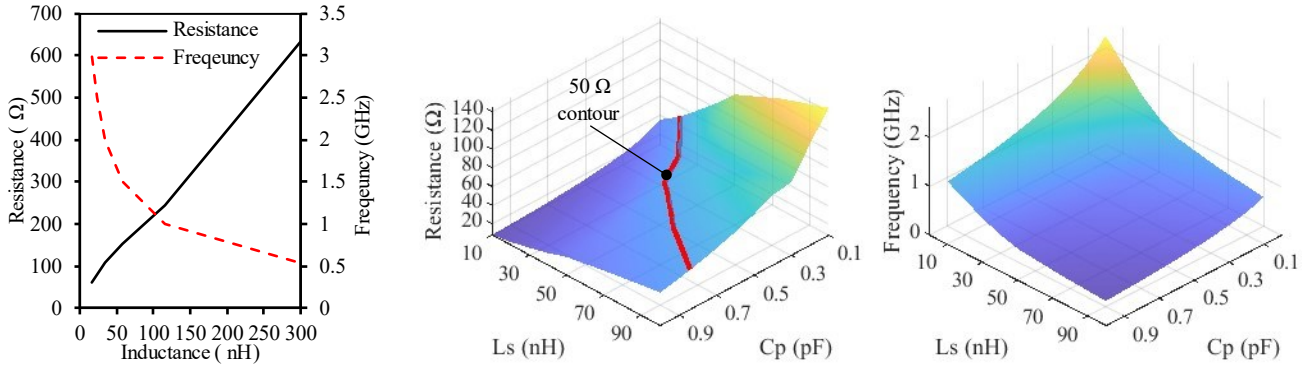

(a) Conventional (b) Proposed

Fig. 3. Input resistance, R_{in}, and frequency of the self-matched branch versus the loading elements when P_{in} = 0 dBm for the conventional (L_a) and proposed (L_s and C_p) cases. In conventional design, diode characteristics as well as the loading determines R_{in}. In the proposed design case, an arbitrary resistance can be achieved by proper loading. In both cases, the input reactance is zero achieving self-matching.

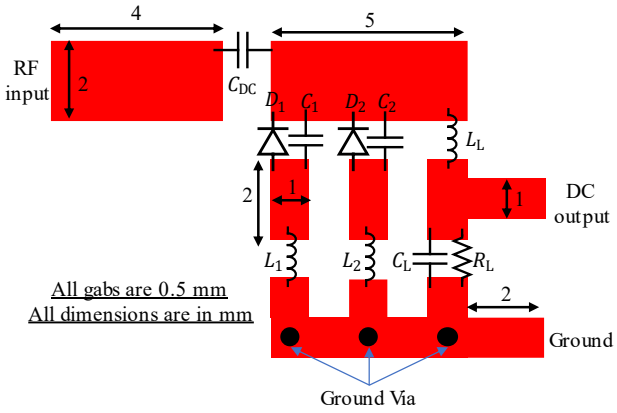

Fig. 4. Layout of the proposed dual-band self-matched rectifier.

TABLE II
OPTIMIZED ELEMENTS OF THE DESIGNED DUAL-BAND RECTIFIER

Element	Value	Unit	Part #
D_1, D_2	-	-	SMS7621-079LF
C_{DC}	56	pF	GQM1875C2E560FB12
L_1	82	nH	LQW15AW82NG80
L_2	36	nH	LQW15AN36NG8Z
C_1	1.3	pF	GJM1555C1H1R3WB01
C_2	0.8	pF	GJM1555C1HR80WB01D
L_L	120	nH	LQW15ANR12J00
C_L	56	pF	GQM1875C2E560FB12
R_L	2	KΩ	-

Rogers RO3003 substrate (height = 0.762 mm, metal thickness = 16 µm, and ε_r = 3) is used in this design. The simulated reflection coefficient of the proposed dual-band rectifier is shown in Fig. 5(a) at two different input powers. These simulation results confirm that the rectifier is matched at two bands 400 MHz and 700 MHz. The PCE is calculated using (9) where P_{in} and V_L are the input RF power, and the dc output voltage, respectively.

$$PCE = V_L^2/(R_L P_{in}) \quad (9)$$

The effect of the quality (Q) factors of the used inductors is studied when the input power was 0 dBm as shown in Fig. 5(b). The higher the Q-factor the better the simulated PCE. The PCE is calculated for two different input powers when the Q-factor is 50 as shown in Fig. 5(c). The PCE is more than 50% for both bands. The Q-factor of 50 represents the approximate value of the Q-factor of the used inductors in Table I at these frequency bands.

Furthermore, in Fig. 5(d), the simulated PCE and output DC voltage are shown versus P_{in} for both frequency bands. In the first band, at 400 MHz, the simulated PCE is more than 50% from -7 dBm to 10 dBm. In the second band, at 700 MHz, the simulated PCE is more than 50% from -5 dBm to 10 dBm and peaks at about 70% at 7 dBm at both bands. Also, in both cases, for $P_{in} \geq 0$ dBm, a load voltage ≥ 1.06 V is achieved.

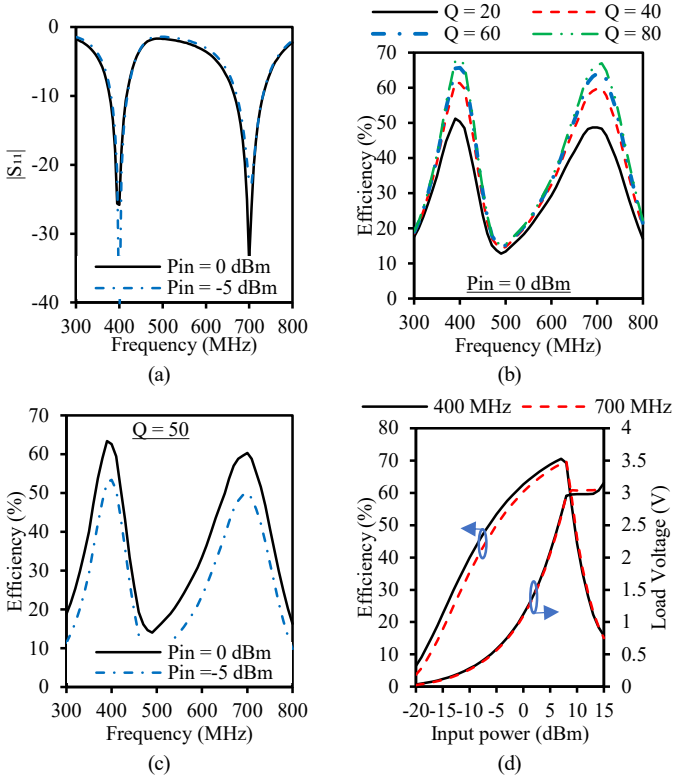

Fig. 5. ADS simulation results of the proposed dual-band self-matched rectifier. (a) reflection coefficient (|S11|). (b) RF-DC PCE varying Q-factor of the inductors at P_{in} = 0 dBm. (c) PCE varying P_{in} for Q = 50. (d) PCE and DC load voltage versus input power assuming inductors have a Q-factor of 50.

III. FABRICATION AND MEASUREMENTS

A. Fabrication and measurement setup

The proposed dual-band self-matched rectifier was fabricated

on Rogers RO3003 based on the design parameters in Table I. The fabricated dual-band self-matched rectifier is shown in Fig. 6. This fabricated dual-band self-matched rectifier has a core area of 0.42 cm^2 (7 mm × 6 mm) and an overall area of 0.7 cm^2 (7 mm × 10 mm) when the area necessary for connecting the RF connector is included. S-parameters measurements were carried out using the Keysight vector network analyzer (part number: N5222A). Also, PCE measurement was performed using a Keysight analog signal generator (part # E8257D) for RF signal generation, and the output voltage was recorded using a multimeter. Then, the PCE was calculated using (9).

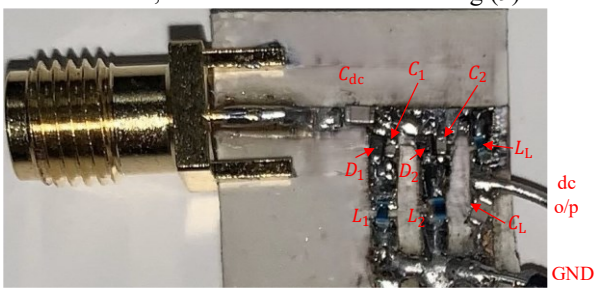

Fig. 6. Photo of the fabricated dual-band rectifier.

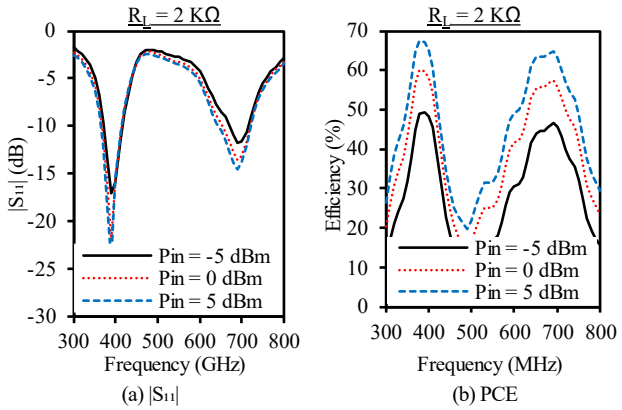

(a) $|S_{11}|$ (b) PCE

Fig. 7. Measurement results of the proposed dual-band rectifier versus frequency.

B. *Measurement Results*

The measured $|S_{11}|$ and PCE versus frequency of the fabricated dual-band rectifier at three different input powers and R_L = 2 KΩ are shown in Fig. 7(a) and 7(b), respectively. The dual-band operation was confirmed at 390 MHz and 690 MHz, which are slightly shifted to lower frequencies than the simulated ones due to the tolerance of the used lumped elements. The PCE varied from 50% to 68% for the 390 MHz band and from 47% to 65% for the 690 MHz band when power changed from -5 to 5 dBm.

Moreover, the simulated and measured PCE versus P_{in} is compared when R_L = 2 KΩ and has a good agreement for both frequency bands as shown in Fig. 8. The measured PCE, for the lower frequency band, was more than 50% when input power changed from -5.5 dBm to 11 dBm as shown in Fig. 8(a). For the upper-frequency band, the measured PCE was more than 50% when the input power ranged from -4 dBm to 12 dBm as shown in Fig. 8(b).

In addition, the measured PCE versus the output load with different input power powers for the lower and upper bands are shown in Fig. 9(a) and 9(b), respectively. In both bands, for an input power of 5 dBm, the measured PCE was more than 50% for 0.5 KΩ < R_L < 3 KΩ and more than 62% for 1 KΩ < R_L < 3 KΩ. At the lower band, the measured RF-DC conversion efficiencies were more than 46%, 50%, 55.5%, and 60% for input power of -5 dBm, -3 dBm, 0 dBm, and 3 dBm, respectively. Also, at the higher band, the measured RF-DC conversion efficiencies were more than 44.5%, 49.5%, 55.6%, and 60.5% for input powers of -5 dBm, -3 dBm, 0 dBm, and 3 dBm, respectively. These results prove the robustness of the proposed technique against the output dc-load variations.

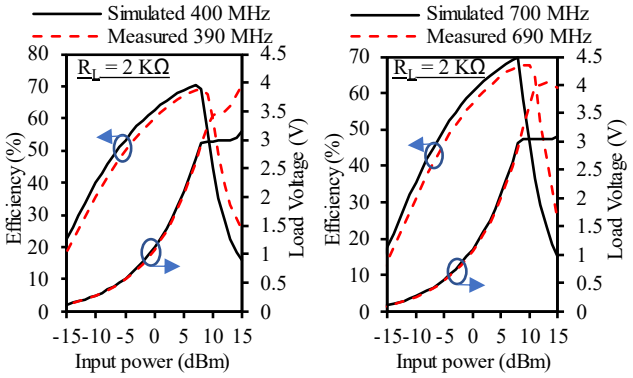

(a) Lower frequency band. (b) Upper frequency band.

Fig. 8. Comparison between simulated and measured results versus input power.

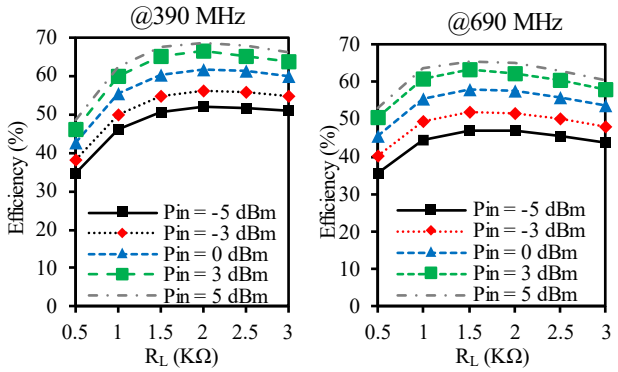

(a) Lower frequency band. (b) Upper frequency band.

Fig. 9. Measured PCE at different input power levels versus load resistance.

C. *Performance comparison*

In Table III, a detailed comparison with other multi-band rectifiers is provided. A very compact size was achieved despite the low frequency of the implementation. It is 3% the size of the design in [1]. However, this is associated with a slightly lower peak PCE when compared to [1]. The reason is the use of lumped inductors with limited Q-factor. Furthermore, the proposed comprehensive self-matching technique enabled an almost equal peak PCE for both bands.

In [6], the peak PCE and the dynamic input power range for PCE > 50% were affected by the level of input resistance which was not exactly 50-Ω at every frequency. Still, our proposed rectifier has an expandability feature like the design in [6]. The dynamic range for PCE > 50% of input power is also comparable to the rectifiers in [1] and [6] and outperforms the rectifier in [7]. Also, the dynamic range for PCE > 60% of input power outperforms the rectifiers in [6] and [7].

TABLE III

PERFORMANCE SUMMARY OF THE PROPOSED RECTIFIER AND COMPARISON WITH STATE-OF-THE-ART MULTI-BAND RECTIFIERS

Reference	Bands	Frequency (GHz)	PCE_{max} (%) @ P_{in} (dBm)	Dynamic P_{in} range (dBm)*		Diode	Size (cm^2)
				PCE >50%	PCE >60%		
This work	**2**	**0.39**	**69 @ 8 dBm**	**-5.5 to 11**	**0 to 10**	**SMS7621**	**0.42**
		0.69	**68 @ 8.5 dBm**	**-4 to 12**	**1 to 11**		
[1]	3	0.895	79.9 @ 9.5 dBm	-5 to 13.5	-1.5 to 12.5	BAT15-03W	15
		2.38	74.6 @ 11 dBm	-3.5 to 13	0.5 to 12.5		
		5.57	73.6 @ 13.5 dBm	1.5 to 16	5 to 15.5		
[6]	2	2.38	67.7 @ 5 dBm	-7 to 11	-2 to 9	BAT15-03W	NR
		4.99	55.3 @ 5 dBm	-2.5 to 9	NA		
	3	1.78	60.9 @ 5 dBm	-5 to 8	2.5 to 6		
		2.35	71.4 @ 5 dBm	-7 to 10	-3 to 8.5		
		4.97	54 @ 5 dBm	0 to 7	NA		
[7]	2	0.915	69.2 @ -1 dBm	-11.8 to 2.5	-6 to 1.5	SMS7630	18.8
		2.45	64.1 @ -1 dBm	-8.6 to 1.7	-4 to -0.5		

*Extracted from curves, NA = Not Applicable, NR = Not reported

V. CONCLUSION

This work presented a compact and efficient dual-band rectifier with self-matched branches. Regardless of the design frequency, comprehensive impedance control was achievable for each branch without affecting the other. The impedance of the self-matched branch was analyzed, and design equations were derived. We demonstrated that this approach provides effective impedance matching for each branch by canceling reactance while allowing for adjustable resistance values. As a proof-of-concept, a dual-band rectifier was fabricated for verification, featuring a core area of 0.42 cm² and an overall area of 0.7 cm² including the RF connector. Measurements confirmed the dual-band operation at 390 MHz and 690 MHz with more than 60% of PCE for input power ranges from 0 to 10 dBm and 1 to 11 dBm, respectively.

REFERENCES

[1] H. Nam, G. T. Bui, D. -A. Nguyen, and C. Seo, "A Compact and High-Efficiency 0.915/2.45/5.8 GHz Triple-Band Rectifier with Harmonic Suppression Based on Coupled Transmission Line," *IEEE Trans. Circuits Syst. II*, *Exp. Briefs*, vol. 71, no. 7, pp. 3553-3557, Jul. 2024.

[2] K. Woo, G. T. Bui, D. -A. Nguyen and C. Seo, "A Compact and High-Efficiency Design of Triple-Band Rectifier with Harmonic Suppression for Wireless Power Transfer," *IEEE Microw. Wireless Compon. Lett*., vol. 34, no. 1, pp. 111-114, Jan. 2024

[3] C. -H. Du, F. Cheng, and C. Gu, "Efficient Tri-Band Rectifier Using Multistub Matching Network for WPT Applications," *IEEE Microw. Wireless Techn. Lett.*, vol. 33, no. 9, pp. 1361-1364, Sept. 2023.

[4] Z. Yue, X. Xu, S. Li, Y. H. Zhu, and X. Q. Lin, "Efficient and Compact Tri-Band Rectifier with Large Frequency Ratio for WPT," *IEEE Microw. Wireless Compon. Lett*., vol. 32, no. 11, pp. 1355-1358, Nov. 2022.

[5] H. Tafekirt, J. Pelegri-Sebastia, A. Bouajaj, and B. M. Reda, "A Sensitive Triple-Band Rectifier for Energy Harvesting Applications," *IEEE Access*, vol. 8, pp. 73659-73664, 2020.

[6] S. H. Wang, S. Y. Zheng, K. W. Leung, and M. H. Xia, "A Self-Matched Multi-Band Rectifier for Efficient Electromagnetic Energy Harvesting," *IEEE Trans. Circuit Syst. I: Reg. Pap.*, vol. 68, no. 11, pp. 4556-4565, Nov. 2021.

[7] J. Liu, M. Huang, and Z. Du, "Design of Compact Dual-Band RF Rectifiers for Wireless Power Transfer and Energy Harvesting," *IEEE Access*, vol. 8, pp. 184901-184908, 2020.

[8] S. Shen, Y. Zhang, C.Y. Chiu, and R. Murch, "A Triple-Band High-Gain Multibeam Ambient RF Energy Harvesting System Utilizing Hybrid Combining," *IEEE Trans. Ind. Electron*., vol. 67, no. 11, pp. 9215-9226, Nov. 2020.

[9] C. Song et al., "Matching network elimination in broadband rectennas for high-efficiency wireless power transfer and energy harvesting," *IEEE Trans. Ind. Electron.*, vol. 64, no. 5, pp. 3950–3961, May 2017.

[10] J. Liu, Y. Z. Xiu, and C. L. Yang, "Analysis and design of dual-band rectifier using novel matching network," *IEEE Trans. Circuits Syst. II*, *Exp. Briefs*, vol. 65, no. 4, pp. 431–435, Apr. 2017.

[11] C. Song *et al*., "A Novel Six-Band Dual CP Rectenna Using Improved Impedance Matching Technique for Ambient RF Energy Harvesting," *IEEE Trans. Antenna Propag.*, vol. 64, no. 7, pp. 3160-3171, Jul. 2016.

[12] X.-B. Huang, J.-J. Wang, X.-Y. Wu and M.-X. Liu, "A dual-band rectifier for low-power wireless power transmission system", in *Proc. Asia–Pacific Microwave Conf.*, Nanjing, China, pp. 1-3, Dec. 2015.

[13] B. Gyawali, M. Aboualalaa, A. Barakat, R. K. Pokharel, "Design of Miniaturized Sub-6 GHz Rectifier with Self-Impedance Matching Technique," *IEEE Trans. Circuits Syst. I: Reg. Papers*, vol. 71, no. 7, pp. 3413-3422, Jul. 2024.

[14] Y. Y. Xiao, J.-H. Ou, S. F. Bo, W. Che, and X. Y. Zhang, "A Simple Technology for Designing Ultrawideband Rectifiers", *IEEE Trans. Microw. Theory Techn.*, vol.72, no.2, pp.1424-1432, 2024.

[15] S. Yu, F. Cheng, C. Gu, C. Wang, and K. Huang, "Compact and Efficient Broadband Rectifier Using T-type Matching Network," *IEEE Microw. Wireless Compon. Lett.*, vol. 32, no. 6, pp. 587-590, Jun. 2022.

[16] B. Gyawali, S. K. Thapa, A. Barakat, K. Yoshitomi, and R. K. Pokharel, "Analysis and design of diode physical limit bandwidth efficient rectification circuit for maximum flat efficiency, wide impedance, and efficiency bandwidths," *Sci. Rep*., vol. 11, Art no. 19941, Oct. 2021.

[17] W. Liu, K. Huang, T. Wang, Z. Zhang, and J. Hou, "A Broadband High-Efficiency RF Rectifier for Ambient RF Energy Harvesting," *IEEE Microw. Wireless Compon. Lett.*, vol. 30, no. 12, pp. 1185-1188, Dec. 2020.

[18] Z. He and C. Liu, "A compact high-efficiency broadband rectifier with a wide dynamic range of input power for energy harvesting," *IEEE Microw. Wireless Compon. Lett.*, vol. 30, no. 4, pp. 433–436, Apr. 2020

[19] P. Wu et al., "Compact high-efficiency broadband rectifier with multistage-transmission-line matching," *IEEE Trans. Circuits Syst. II, Exp. Briefs,* vol. 66, no. 8, pp. 1316–1320, Aug. 2019.

[20] S. Zheng, W. Liu, and Y. Pan, "Design of an Ultra-Wideband High-Efficiency Rectifier for Wireless Power Transmission and Harvesting Applications," *IEEE Trans. Ind. Informat.*, vol. 15, no. 6, pp. 3334-3342, Jun. 2019.

[21] M. Huang et al., "Single- and Dual-Band RF Rectifiers with Extended Input Power Range Using Automatic Impedance Transforming," *IEEE Trans. Microw. Theory Techn.*, vol. 67, no. 5, pp. 1974-1984, May 2019.

[22] P. Wu, S. Y. Huang, W. Zhou, and C. Liu, "One Octave Bandwidth Rectifier with a Frequency Selective Diode Array," *IEEE Microw. Wireless Compon. Lett.*, vol. 28, no. 11, pp. 1008-1010, Nov. 2018.

[23] Y. L. Lin, X. Y. Zhang, Z. -X. Du, and Q. W. Lin, "High-Efficiency Microwave Rectifier with Extended Operating Bandwidth," *IEEE Trans. Circuit Syst. II: Exp. Briefs*, vol. 65, no. 7, pp. 819-823, Jul. 2018.

[24] M. M. Mansour and H. Kanaya, "Compact and Broadband RF Rectifier With 1.5 Octave Bandwidth Based on a Simple Pair of L-Section Matching Network," *IEEE Microw. Wireless Compon. Lett.*, vol. 28, no. 4, pp. 335-337, Apr. 2018.